Synthesis, Ionisation Potentials and Electron Affinities of Hexaazatrinaphthylene Derivatives

Stephen Barlow,[a, b] Qing Zhang,[a] Bilal R. Kaafarani,[a, b, c] Chad Risko,[a] Fabrice Amy,[d] Calvin K. Chan,[d] Benoit Domercq,[e] Zoya A. Starikova,[f] Mikhail Yu. Antipin,[f, g] Tatiana V. Timofeeva,[g] Bernard Kippelen,[e] Jean-Luc Brédas,[a] Antoine Kahn,[d] and Seth R. Marder*[a, b]

Abstract: Several hexaazatrinaphthylene derivatives and a tris-(thieno)hexaazatriphenylene derivative have been synthesised by reaction of the appropriate diamines with hexaketocyclohexane. The crystal structure of 2,3,8,9,14,15-hexachloro-5,6,11,12,17,18-hexaazatrinaphthylene has been determined by X-ray diffraction; this reveals a molecular structure in good agreement with that predicted by density functional theory (DFT) calculations and π-stacking with an average spacing between adjacent molecular planes of 3.18 Å. Solid-state ionisa-tion potentials have been measured by using UV photoelectron spectroscopy and fall in the range of 5.99 to 7.76 eV, whereas solid-state electron affinities, measured using inverse photoelectron spectroscopy, vary in the range −2.65 to −4.59 eV. The most easily reduced example is a tris(thieno)hexaazatriphe-nylene substituted with bis(trifluoro-methyl)phenyl groups; DFT calcula-tions suggest that the highly exother-mic electron affinity is due both to the replacement of the outermost phenyl-ene rings of hexaazatrinaphthylene with thieno groups and to the presence of electron-withdrawing bis(trifluoro-methyl)phenyl groups. The rather exo-thermic electron affinities, the potential for adopting π-stacked structures and the low intramolecular reorganisation energies obtained by DFT calculations suggest that some of these molecules may be useful electron-transport mate-rials.

Keywords: electron affinities · electron transport · heterocycles · ionization potentials · pi stacking

Introduction

Derivatives of 5,6,11,12,17,18-hexaazatrinaphthylene (diquinoxalino[3,3-*a*:2′,3′-*c*]phenazine, **1**) have recently attracted attention as materials for organic electronic applications. These compounds can, depending on the choice of substituent, form films with a wide range of morphologies, including crystalline, columnar discotic liquid-crystalline and amor-

[a] Dr. S. Barlow, Dr. Q. Zhang, Dr. B. R. Kaafarani, Dr. C. Risko, Prof. J.-L. Brédas, Prof. S. R. Marder
School of Chemistry and Biochemistry and
Center for Organic Photonics and Electronics
Georgia Institute of Technology, Atlanta, GA 30332 (USA)
Fax: (+1) 404-894-5909
E-mail: seth.marder@chemistry.gatech.edu

[b] Dr. S. Barlow, Dr. B. R. Kaafarani, Prof. S. R. Marder
Department of Chemistry
University of Arizona, Tucson, AZ 85721 (USA)

[c] Dr. B. R. Kaafarani
Current address:
Department of Chemistry
American University of Beirut, Beirut (Lebanon)

[d] Dr. F. Amy, C. K. Chan, Prof. A. Kahn
Department of Electrical Engineering
Princeton University, Princeton, NJ 08544 (USA)

[e] Dr. B. Domercq, Prof. B. Kippelen
School of Electrical and Computer Engineering and
Center for Organic Photonics and Electronics
Georgia Institute of Technology, Atlanta, GA 30332 (USA)

[f] Dr. Z. A. Starikova, Prof. M. Y. Antipin
Institute of Organoelement Compounds
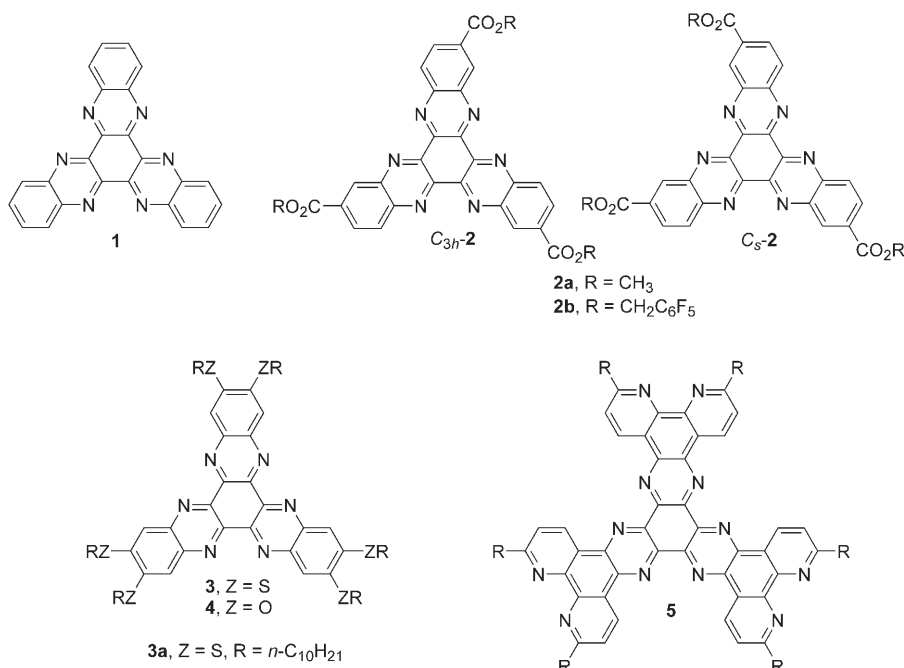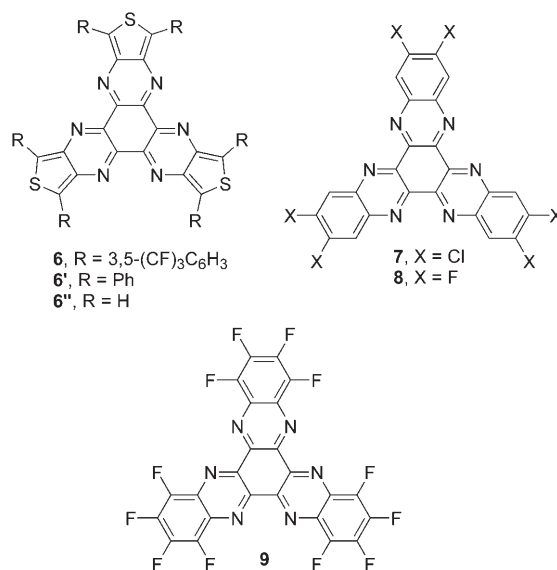Russian Academy of Sciences, Moscow (Russia)

[g] Prof. M. Y. Antipin, Prof. T. V. Timofeeva
Department of Natural Sciences
New Mexico Highlands University, Las Vegas, NM 87701 (USA)

📖 Supporting information for this article is available on the WWW under http://www.chemeurj.org/ or from the author.

phous. Most work has concerned esters derived from the 2,8,14- and 2,8,15-tricarboxylic acid (**2**)[1,2] or 2,3,8,9,14,15-hexa(alkylsulfanyl) (**3**)[3–6] and 2,3,8,9,14,15-hexa(alkoxy) derivatives (**4**).[7,8] Analogues with more extensive π-systems, such as **5**, have also been reported.[9]

One-dimensional charge-carrier mobilities have been obtained by using the pulse-radiolysis time-resolved microwave conductivity technique for the crystalline and liquid-crystalline phases formed by the hexa(alkylsulfanyl) derivatives (**3**),[4,6] with the largest value so far, 0.9 cm^2 V^{-1} s^{-1}, being found at 85°C for crystalline **3a** (R = n-C$_{10}$H$_{21}$);[6] this technique measures the sum of hole and electron mobilities and computational work suggests that both carriers contribute to the observed mobility in these materials.[4] Recently we investigated the pentafluorobenzyl triester, **2b**, and, using the space-charge limited current technique, determined mobilities of 0.07 and 0.02 cm^2 V^{-1} s^{-1} for the C_s isomer and as-synthesised isomer mixture, respectively.[2] Energy-level considerations based on electrochemical measurements suggest that hexaazatrinaphthylene derivatives are likely to function as electron-transport materials and that the mobilities we reported for **2b** in reference [2] are likely to represent electron mobilities. Further support for the ease of electron injection relative to hole injection comes from direct measurements of the solid-state ionisation potentials (IPs) of **1**[2] and

to be −4.59 eV, considerably more exothermic than that of **1**.[10] In addition, this material can be n-doped with cobaltocene, which greatly enhances electron injection into the material.[10]

6, R = 3,5-(CF$_3$)$_2$C$_6$H$_3$
6', R = Ph
6'', R = H

7, X = Cl
8, X = F

9

1

C_{3h}-**2**

C_s-**2**

2a, R = CH$_3$
2b, R = CH$_2$C$_6$F$_5$

3, Z = S
4, Z = O

3a, Z = S, R = n-C$_{10}$H$_{21}$

5

In this paper we report more fully on the solid-state photoelectron (PES) and inverse-photoelectron (IPES) spectra of **1** and **6** and compare these with the PES and IPES spectra of the halogenated hexaazatrinaphthylenes **7** and **9** and of a representative example of the hexa(alkylsulfanyl)hexaazatrinaphthylenes, **3a**. The experimental results are compared to quantum-chemical estimates for these and additional compounds. Furthermore, we report the syntheses of **6** and **9** for the first time, along with the crystal structure of **7**; the π-stacking seen in this structure suggests that vapour-deposited **7** may be an interesting charge-transport material.

3a[5] as 6.6 and 5.9 eV, respectively, and of the solid-state electron affinity (EA) of **1** as −2.4 eV.[2] Recently, we reported the EA of tris{2,5-bis(3,5-bis-trifluoromethyl-phenyl)-thieno}[3,4-b,h,n]-1,4,5,8,9,12-hexaazatriphenylene (**6**; i.e., an analogue of a hexaazatrinaphthylene in which the outer benzene rings are replaced with thiophene rings fused to the hexaazatriphenylene core through their 3- and 4-positions)

Results and Discussion

Synthesis: Compounds **1** and **7–9** were synthesised from reaction of the appropriate o-phenylene diamine with hexaketocyclohexane octahydrate in the presence of acetic acid (Scheme 1).[11,12] The diamines were either commercially
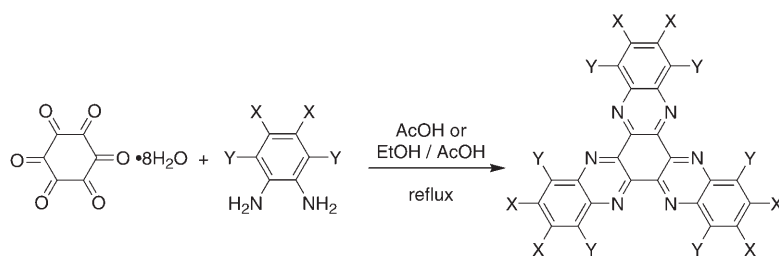
Scheme 1. General synthesis of hexaazatrinaphthylene derivatives used for the preparation of **1** (X=Y=H), **7** (X=Cl, Y=H), **8** (X=F, Y=H) **9** (X=Y=F).

graphic symmetry (C_1), molecules of **7** appear highly symmetrical, with approximate D_{3h} symmetry.

Table 1 summarises the key bond lengths (averaged over chemically equivalent bonds for each structure), defined according to Figure 2, from the structures of two chloroform

available (for **1** and **7**) or were synthesised using literature procedures (for **8** and **9**).[13–16] Compound **3a** was obtained from **7** according to the literature procedure.[6] These compounds were very poorly soluble in organic solvents and were, therefore, purified by gradient sublimation under high vacuum.[17] The fluorinated derivatives **8** and **9** were especially insoluble and ^{1}H and ^{19}F NMR spectra could only be obtained in the presence of strong acids (trifluoroacetic acid or sulfuric acid).

Compound **6** was obtained in an analogous fashion to the hexaazatrinaphthylene derivatives from the reaction of hexaketocyclohexane octahydrate with the diamine **S3** (Scheme 2), which was in turn obtained from the corresponding dinitro compound **S2**, which was synthesised using the Stille coupling of 2,5-dibromo-3,4-dinitrothiophene (**S1**) and 3,5-bis(trifluoromethyl)phenyltributylstannane. As might be anticipated from the presence of the bis(trifluoromethyl)phenyl substituents, **6** is more soluble in common organic solvents than **7–9** and could, therefore, be purified by column chromatography.

Molecular geometry: Crystals of 2,3,8,9,14,15-hexachloro-5,6,11,12,17,18-hexaazatrinaphthylene (**7**) suitable for X-ray structure determination were obtained from gradient vacuum sublimation. Crystallographic data and details of the crystal structure solution and refinement are given in the Experimental Section, with complete information provided in the Supporting Information; the molecular structure is shown in Figure 1. As in the previously reported structures of the solvates of **1**,[12,18] the molecules are essentially planar (mean deviation of the C and N atoms from the RMS molecular plane of 0.038 Å) and, despite low crystallo-
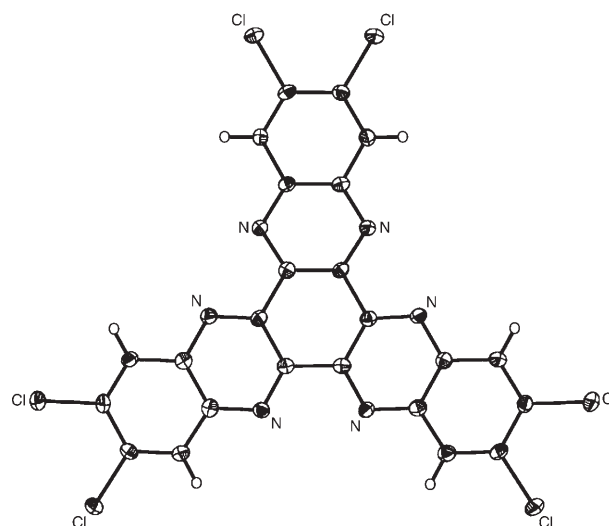
Figure 1. Molecular structure of 2,3,8,9,14,15-hexachloro-5,6,11,12,17,18-hexaazatrinaphthylene (**7**) from X-ray crystallography.

solvates of **1**[12,18,19] and from that of **7**. Also included in Table 1 are the corresponding bond lengths from density functional theory (DFT) calculations (B3LYP/6–31G**) for the gas-phase molecules of **1**, **6–9** and for the related model compounds benzene (**I**), pyrazine (**II**), triphenylene (**III**) and 1,4,5,8,9,12-hexaazatriphenylene (**IV**; Figure 2). The table shows that the computational geometries are in good agreement with the three experimental structures and that the structural difference between **1** and **7** and the other hexaazatrinaphthylene derivatives are relatively minor. Several resonance forms can be envisaged for hexaazatrinaphthylenes; two of these are indicated in Figure 2 and differ in
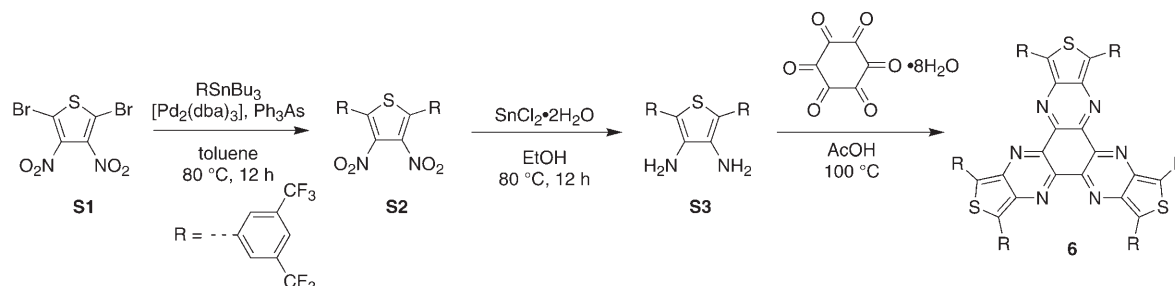
Scheme 2. Synthetic route for compound **6**.

Table 1. Key bond lengths [defined in Figure 2 in Å] from B3LYP-31G** DFT calculations and X-ray crystallography (in italics) for the π-systems of hexaazatrinaphthylenes and related structures.

	I	II	III	IV	1·CHCl₃[12]	1·4CHCl₃[18]	1	Cs-2a[a]	6	6′	6″	7	7	8	9
a	–	–	1.467	1.465	*1.477(3)*	*1.479(6)*	1.478	1.478	1.478	1.478	1.483	*1.474(6)*	1.477	1.477	1.477
b	1.396	1.338	1.421	1.417	*1.424(4)*	*1.425(2)*	1.439	1.439	1.453	1.453	1.459	*1.427(6)*	1.438	1.436	1.438
c	1.396	1.396	1.413	1.348	*1.328(1)*	*1.325(2)*	1.324	1.323–1.324	1.318	1.318	1.316	*1.322(2)*	1.324	1.325	1.323
d	–	–	1.383	1.325	*1.360(1)*	*1.359(6)*	1.353	1.352–1.353	1.355	1.355	1.359	*1.351(1)*	1.351	1.349	1.346
e	–	–	1.401	1.407	*1.419(4)*	*1.424(7)*	1.434	1.434	1.449	1.452	1.451	*1.423(3)*	1.431	1.437	1.438
f	–	–	–	–	*1.414(1)*	*1.413(2)*	1.421	1.418–1.421	1.401	1.402	1.386	*1.412(1)*	1.418	1.422	1.421
g	–	–	–	–	*1.359(3)*	*1.371(13)*	1.375	1.373–1.380	1.736	1.739	1.718	*1.363(1)*	1.375	1.367	1.375
h	–	–	–	–	*1.405(3)*	*1.414(6)*	1.422	1.427	–	–	–	*1.426(2)*	1.432	1.424	1.418

[a] For this compound, the reduced symmetry means there is more than one chemically inequivalent type of c, d, f and g bond length. Very similar bond lengths are found for Cs-2b.
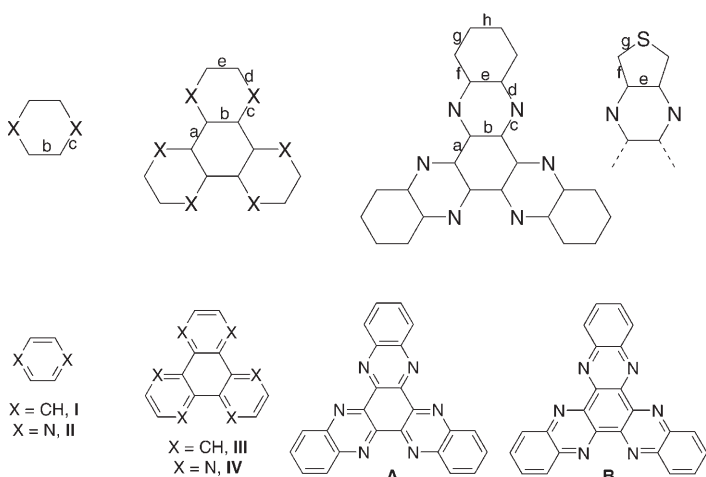

Figure 2. Top: general structures of arenes, triphenylenes, hexaazatrinaphthylenes and tris(thieno)hexaazatriphenylenes showing labelling of chemically inequivalent bonds as used in Table 1. Below: structures of benzene (**I**), pyrazine (**II**), triphenylene (**III**) and hexaazatriphenylene (**IV**) and two of the resonance structures possible for hexaazatrinaphthylenes.

which of the six-membered rings is formally "aromatic". While no single resonance structure adequately accounts for the pattern of bond lengths, structures of type **A** (Figure 2) are clearly important, as suggested by: the shortest bonds being between the central six-membered ring and the nitrogen atoms (c, Figure 2); the bonds between the nitrogen atoms and the outermost rings (d) being somewhat longer than c; and the bonds within the central ring (a and b) being very long. This picture is similar to that calculated for triphenylene (**III**) or hexaazatriphenylene (**IV**) in that the central ring has rather long bonds; however, these bonds are longer in the hexaazatrinaphthylenes, while the c bonds are shorter and the relative lengths of c and d bonds are reversed. The bond lengths calculated for the tris-(thieno)hexaazatriphenylenes, **6**, **6′** and **6″**, suggest that **A**-type resonance structures dominate even more strongly in these compounds; in particular, the c bonds are slightly shorter and the b and d bonds are slightly longer than the corresponding bonds in the hexaazatrinaphthylenes. These observations can be rationalised by using a simple valence-bond picture; only a single resonance structure (analogous

to structure **A** shown above for hexaazatrinaphthylenes) can be drawn for the thieno species without separating charges. Accordingly, the bond lengths in the thiophene rings of **6**, **6′** and **6″** show similar patterns to that of thiophene (at the same level of theory S−C, C=C and C−C bond lengths are 1.735, 1.367 and 1.429 Å, respectively), with the differences between the different compounds presumably arising from steric effects associated with the aryl groups. These steric effects also result in a deformation of the core π-systems of **6** and **6′**; a slight twist of the arms reduces the steric interactions between the substituted aryl groups of neighbouring arms.

Orbital structure, radical anion and cation geometries, and reorganisation energies: We have also calculated the geometries of the radical cations and anions of **1**, Cs-**2a**, Cs-**2b**, **6′**, **6″** and **7–9**;[20] full details are given in the Supporting Information. Reduction of **1** leads to moderate bond-length changes throughout the structure while maintaining D_{3h} symmetry; the largest changes are decreases of 0.010 Å in the h bond lengths and increases of 0.008, 0.009 and 0.009 Å in the c, d and g bond lengths, respectively, consistent with the bonding or antibonding character of the LUMO across the bonds in question. The LUMO of **1** (Figure 3) has a_2'' symmetry and is qualitatively similar to that previously reported for **3** (R = H).[6] Qualitatively similar LUMOs are obtained for Cs-**2a**, Cs-**2b**, **6′**, **6″** and **7–9**, with the addition of small coefficients on the π-accepting carbonyl groups of the ester derivatives **2a** and **2b** (see Supporting Information for reference [2]). The calculated changes in the bond lengths between the neutral molecule and the radical anion for compounds **2a**, **2b**, **6′**, **6″** and **7–9** are similar to those for **1**.

The B3LYP/6-31G** HOMO of **1** (Figure 3) is a doubly degenerate orbital of e″ symmetry, as is the previously reported qualitatively similar HOMO calculated for **3** (R = H),[5] while the non-degenerate HOMO−1 has a_1'' symmetry. Accordingly, the structure of **1**⁺, in which an electron is removed from one of these degenerate orbitals, is subject to Jahn–Teller distortion. The optimised structure for the cation does indeed lack the D_{3h} symmetry of the neutral molecule; the most dramatic bond-length changes are the shortening of two of the c type bonds by 0.017 Å, one in each of two arms (see Supporting Information for full details). The hexahalo derivatives **7** and **8** also have degener-
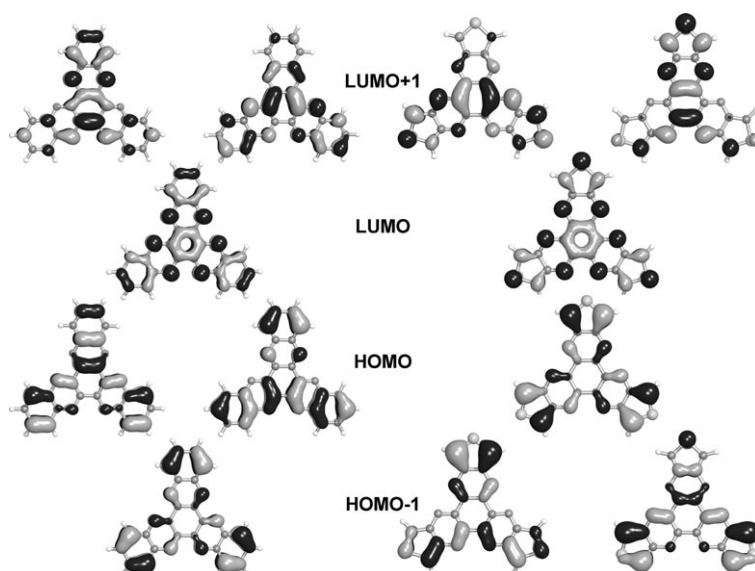
Figure 3. Frontier orbitals calculated at the B3LYP/6-31G** level for **1** (left) and **6″** (right).

sum of λ_1, the energy corresponding to relaxation on the neutral potential-energy surface from the radical-ion state geometry to the relaxed neutral geometry and λ_2, the relaxation on the radical-ion potential energy surface from the neutral geometry to the relaxed radical-ion geometry; the calculated values are given in Table 2. There is not a particularly clear dependence of the reorganisation energy on chemical structure, although for **1**, **7** and **8**, in which the radical cations are Jahn–Teller distorted (vide supra), the values for hole transfer exceed those

ate HOMOs and undergo Jahn–Teller distortion on oxidation. However, in the dodecafluoro species, **9**, the a_1'' orbital is the HOMO, albeit only 0.03 eV higher in energy than the e″ degenerate HOMO-1; accordingly, **9**·+ retains D_{3h} symmetry. The general appearance of the a_1'' and e″ orbitals is very similar for the halogenated derivatives and for **1**, although out-of-phase contributions from the π-donor halogen atoms are seen in **7–9**. In the case of C_s-**2a** and C_s-**2b**, the HOMO is related to that of **1** (see Supporting Information for reference [2]); inevitably the low symmetry of the substitution factor means the degeneracy is lifted, albeit by only 0.02–0.03 eV, and oxidation leads to Jahn–Teller-like distortion similar to that seen for **1**·+. The tris-(thieno)hexaazatriphenylene derivatives **6**, **6′** and **6″** show broadly similar frontier orbitals to the hexaazatrinaphthylene derivatives (shown for **6″** in Figure 3; orbitals for **6** are shown in the Supporting Information and are broadly similar, with only small coefficients on the aryl groups). The frontier orbital ordering in **6**, **6′** and **6″** is the same as that in **9**, but with a larger separation between the non-degenerate HOMO and the degenerate HOMO−1 and, accordingly, **6′**·+ and **6″**·+ are predicted to retain threefold symmetry.

The geometric changes associated with oxidation and reduction determine the intramolecular components of the reorganisation energies for the electron-exchange reactions between the neutral molecules and their radical cations and anions and, therefore, the barrier to hole or electron transport between molecules in the solid state. According to Marcus theory[21] and as shown pictorially elsewhere,[22] this barrier is λ/4, in which λ is the sum of the internal reorganisation energy (λ_i) and external reorganisation energy (λ_s), which is associated with changes in polarisation and positions of the surrounding molecules. We have used B3LYP/6-31G** calculations to evaluate λ_i for hole and electron transfer for **1**, **2a**, **2b**, **6′**, **6″**, **7**, **8** and **9** from the adiabatic potential surfaces.[20,23] Specifically, we calculated λ_i as the

Table 2. Intramolecular reorganisation energies [eV] for hole and electron exchange calculated at the B3LYP/6–31G** level.[a]

	cation/neutral			neutral/anion		
	λ_1	λ_2	λ_i	λ_1	λ_2	λ_i
1	0.074	0.063	0.137	0.048	0.047	0.095
2a	0.102	0.096	0.198	0.087	0.083	0.170
2b	0.056	0.052	0.108	0.100	0.096	0.196
6′	0.038	0.039	0.078	0.061	0.067	0.129
6″	0.035	0.033	0.068	0.046	0.044	0.091
7	0.083	0.075	0.158	0.058	0.058	0.117
8	0.100	0.097	0.197	0.076	0.077	0.153
9	0.087	0.083	0.169	0.082	0.082	0.164

[a] The total intramolecular reorganisation energy, λ_i, is the sum of the relaxation energies of the neutral molecule, λ_1 and of the charged species, λ_2, on electron transfer.

for electron transfer. However, in general, the reorganisation energies for both hole and electron transfer are rather small compared to those calculated at the same level of theory for many other commonly used transport materials. For example, a value of 0.29 eV was reported for TPD·+/TPD {TPD = N,N′-diphenyl-N,N′-di(m-tolyl)(biphenyl-4,4′-diamine)},[24] 0.28 eV for AlQ₃/AlQ₃·⁻ {AlQ₃ = tris(8-hydroquinolato)aluminium},[25] and 0.38–0.61 and 0.49–0.56 eV for hole and electron exchange, respectively, in 1,1-diaryl-2,3,4,5-tetraphenylsiloles.[26] Indeed, the reorganisation energy of 0.091 eV calculated for **6″**·+/**6″** is even smaller than that calculated for pentacene·+/pentacene (0.098 eV); the reorganisation energy of 0.068 eV for **6″**/**6″**·⁻ is even lower. These values are consistent with the high mobilities that have been reported in some hexaazatrinaphthylene derivatives.[2,4,6]

Packing in the structure of compound 7: The electronic properties of molecular transport materials depend on the manner in which the molecules are organised in the solid state.[27–29] In particular, π-stacking, although not a guarantee

of good wavefunction overlap,[30] is a feature of many high mobility materials, including many columnar discotic liquid-crystalline mesophases,[31,32] including hexaazatrinaphthylene derivatives,[6,8] phthalocyanines and perylene-based materials,[33] polythiophenes,[34] extended porphyrins[35] and some pentacene derivatives.[36] Both molecular sheets and molecular π-stacks are found in the crystal structure of **7**. The structure can be described in terms of molecular sheets parallel to the (102) crystallographic plane; Figure 4 shows the top
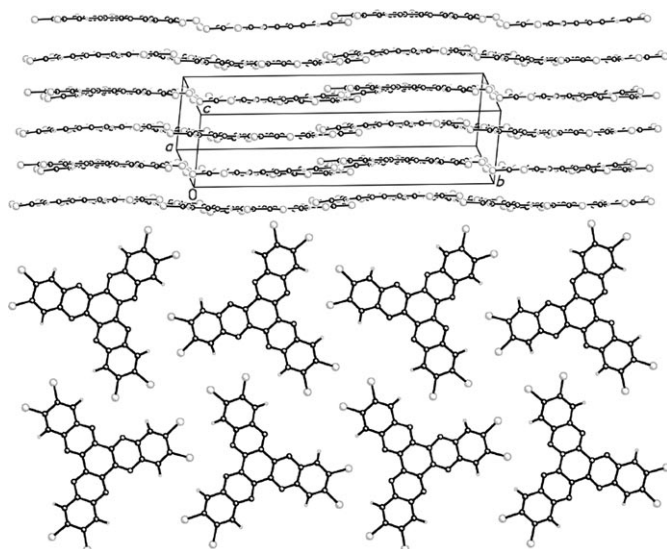

Figure 4. Two views of the molecular packing in crystals of **7** emphasizing its description in terms of sheets of molecules. The lower view is along the (102) direction.

Figure 5. Two views of the π-stacked columns in the structure of **7**.

view and side views of these sheets, the latter revealing they are slightly corrugated with the molecular planes deviating from the mean plane of the sheet. Within the sheets there are some short intermolecular Cl···Cl, N···Cl and C···H contacts (as short as 3.323, 3.232 and 2.781 Å, respectively; see Supporting Information for details). There is also a large number of intersheet contacts (see Supporting Information); molecules in successive sheets form slipped stacks propagating along the crystallographic z axis. Figure 5 shows two views of how the molecules are arranged in the stacks, with the average spacing between adjacent molecular planes being 3.18 Å. This π-stacking distance is somewhat shorter than seen in π-stacks of **1**·CHCl$_3$ (3.48 Å);[12] the structure of **1**·4CHCl$_3$ is quite different, with π-interactions within centrosymmetric dimers with an interplanar distance of 3.31 Å.[18] It is also rather short compared to the corresponding distance in many other π-stacked organic electronic materials,[36–41] including discotic columnar hexaazatrinaphthylene materials such as **3a**[6] and **4**.[8] However, an equally short π-stacking distance of 3.18 Å has been reported in a high-carrier-mobility hydrogen-bonded hexaazatriphenylene-based columnar material.[42]
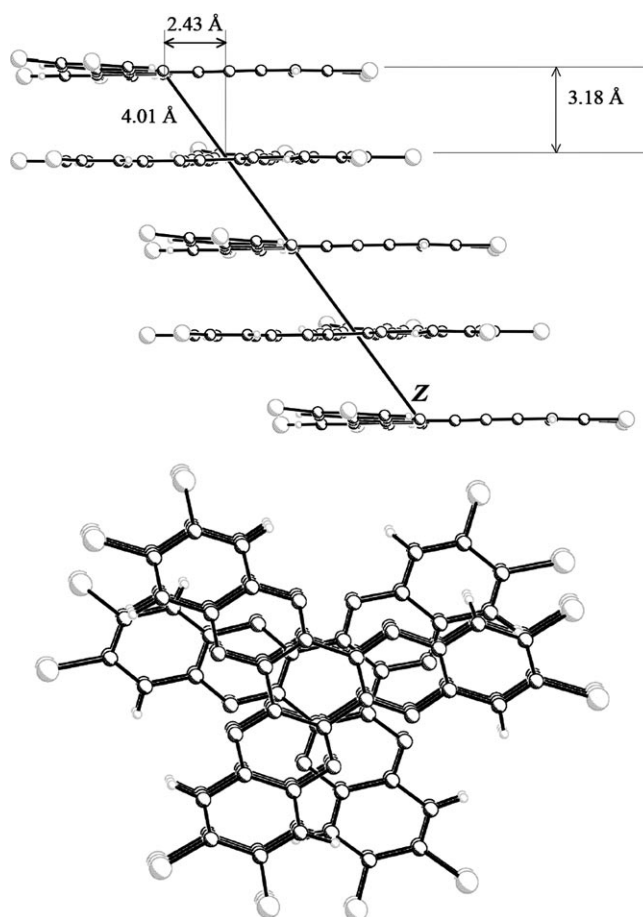
Ionisation potential and electron affinity: When considering the use of an organic material for charge-transport applications it is important to have an understanding of its solid-state ionisation potentials (IPs) and electron affinities (EAs). This understanding can help in identifying suitable partner organic transport materials and inorganic electrode materials and in establishing whether holes or electrons are dominant carriers in a particular device situation. Estimates have often been made based on comparison of the electrochemistry, sometimes in conjunction with optical data, of the species of interest with that of compounds of known IP and/or EA. Aside from the uncertainties arising from the assumptions involved in these estimates,[43] complications may arise due to the presence of aggregates, which NMR spectroscopy suggests are present for **2b**[2] and species of type **3**[6] at the concentrations typically employed for electrochemical measurements. Moreover, some of the halogenated hexaazatrinaphthylenes are insufficiently soluble for electrochemical investigations.

In contrast, photoelectron spectroscopy (PES) and inverse-photoelectron spectroscopy (IPES) of solid films provide direct measures of IP and EA, respectively. We acquired PES and IPES data for vacuum-deposited films of **1**, **6**, **7** and **9** and for a spin-coated film of one of the hexa(alkylsufanyl) class of materials, **3a**, for comparison. The PES

and IPES spectra are shown in Figure 6; in general, qualitatively similar densities of states are observed for **1**, **6**, **7** and **9**, consistent with the qualitatively similar orbital pictures suggested by our calculations (the small HOMO/HOMO−1 splittings are not resolved in the PES spectra). The PES spectra for **3a** look rather different, being dominated by an intense feature with a peak corresponding to an IP greater than 10 eV (binding energy vs. E_F of about −6 eV) which dwarfs and/or obscures some of the hexaazatrinaphthylene ionisations. This is similar to previously reported PES spectra for **3** (R=C₆H₁₃, here the ratio of intensities between the >10 eV feature and the lowest energy ionisation is somewhat reduced)[5] and also to spectra of silicon-bound alkyl monolayers (see Supporting Information for comparison of the PES of **3a** and one of these monolayers);[44,45] in all these systems the intense feature is presumably due to ionisations from the side chains. In both cases, however, the lowest energy IP attributed to ionisation from the HOMO can be resolved; our value of the corresponding adiabatic IP for the lowest energy ionisation of **3a** is in good agreement

with the value of 5.9 eV previously reported for its hexyl analogue.[5] The adiabatic IPs and EAs, extracted from the PES and IPES spectra, respectively, are given in Table 3, along with DFT estimates of the adiabatic and vertical gas-phase IPs and EAs. The computed values follow the experimental trends, although, as expected, they are consistently more endothermic than the observed values. Solid-state IPs are known to be as much as 1–1.5 eV lower than experimental gas-phase values, due to stabilisation of the cation by polarisation of the surrounding molecules in the solid,[46,47] and analogous effects can be anticipated to make the solid-state EA values more exothermic than gas-phase values. In addition, π-stacking effects may affect the solid-state spectra, as previously noted for PES spectra of **3** (R=C₆H₁₃).[5]

The solid-state IPs are all higher than those of the widely used hole-transport materials, TPD[47] and NPD {NPD = N,N'-diphenyl-N,N'-di(1-naphthyl)(biphenyl-4,4'-diamine)} (5.5 eV).[48,49] With the exception of **3a**, the IPs are also in excess of that of the commonly used electron-transport material AlQ₃ (5.93 eV),[47] suggesting they should be more effective as "hole-blocking" materials.

The EA of **1** is somewhat more exothermic than that of the widely used electron-transport material, AlQ₃ (−2.0 to −2.5 eV)[50] and also more exothermic than those measured for 1,1-diaryl-2,3,4,5-tetraphenylsiloles (−1.5 to −2.4 eV).[26] As one would expect, the halogenated derivatives **7** and **9** are both significantly more easily reduced and less readily oxidised than the parent heterocycle, the IPs and EAs between the halogenated and non-halogentated materials differing by around 1 eV. The similarity of the experimental EAs of **7** and **9** might appear surprising at first sight, given the greater electronegativity of fluorine relative to that of chlorine (Pauling electronegativities are 3.98 and 3.16, respectively[51]). However, this result closely parallels IPES data showing films of 1,3,5-trichlorobenzene and hexafluorobenzene to have rather similar EAs;[52] thus, in both that study and ours twice as many fluorine substituents are required to affect the EA to the same extent as chlorine substituents, presumably reflecting the inter-
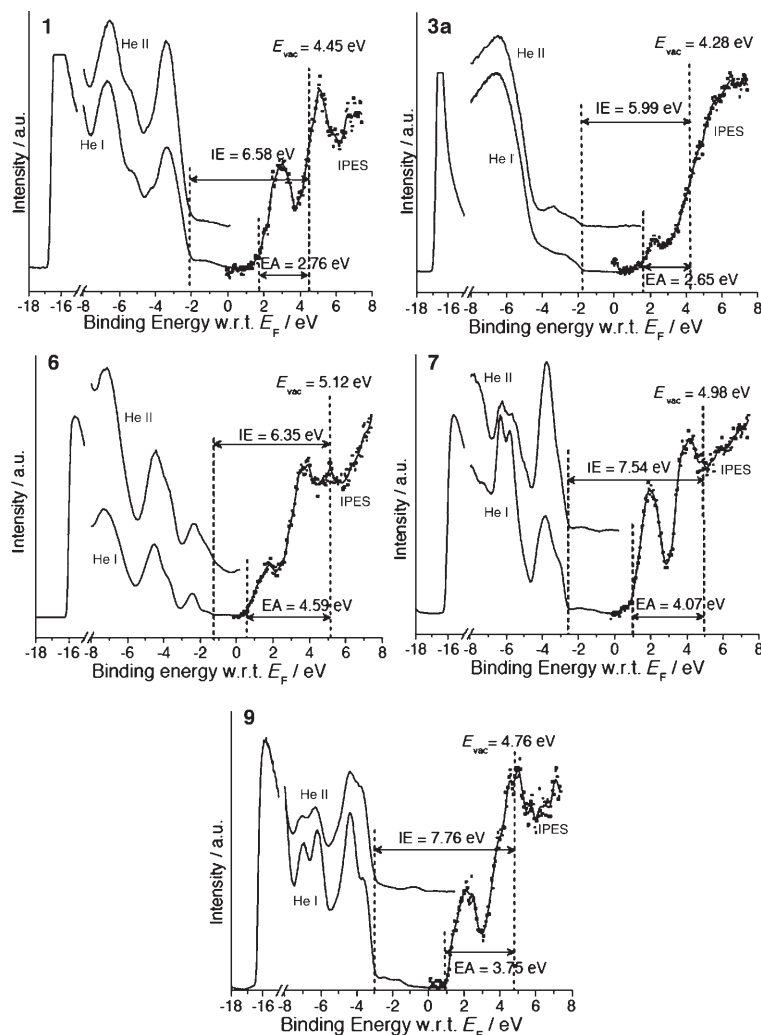

Figure 6. PES and IPES spectra for some hexaazatrinaphthylene and tris(thieno)hexaazatriphenylene derivatives.

Table 3. Adiabatic ionisation potentials (IPs) and electron affinities (EAs) for some hexaazatrinaphthylene derivatives obtained using PES and IPES, together with adiabatic and vertical values from B3LYP/6-31G** calculations.

| | IP [eV] | | | EA[a] [eV] | | |
| | PES | DFT | | IPES | DFT | |
	adiabatic	vertical	adiabatic	adiabatic	vertical	adiabatic
1	6.58 ± 0.1	7.63	7.56	-2.76 ± 0.4	-1.40	-1.45
2a	–	7.82	7.72	–	-1.89	-1.97
2b	–	7.83	7.78	–	-2.09	-2.19
3a	5.99 ± 0.1	–	–	-2.65 ± 0.4	–	–
6	6.35 ± 0.1	7.04	[b]	-4.59 ± 0.4	-3.08	[b]
6′	–	6.08	6.04	–	-2.20	-2.27
6″	–	7.24	7.20	–	-1.78	-1.82
7	7.54 ± 0.1	7.98	7.91	-4.07 ± 0.4	-2.19	-2.25
8	–	7.97	7.87	–	-1.80	-1.88
9	7.76 ± 0.1	8.12	8.04	-3.75 ± 0.4	-2.22	-2.30

[a] We have used the definition of EA as the energy change for the process $M + e^- \rightarrow M^{\cdot-}$; hence the negative values indicate exothermicity for the reduction of a molecule. [b] Not calculated.[20]

play of σ-acceptor and π-donor effects (fluorine is both a better σ-acceptor and π-donor than chlorine in organic systems).[53] Moreover, the calculated gas-phase data also suggests similar EAs for **7** and **9**, these values being more exothermic than that calculated for the hexafluoro derivative, **8**.

The most easily reduced material, according to the EA measurements, is the tris(thieno)hexaazatriphenylene compound, **6**, the EA of which is approximately 0.5 eV more exothermic than that of **7** (around 1.8 eV more exothermic than that of the parent **1**). Indeed, it is this highly exothermic EA that prompted us to carry out n-type doping of this material with cobaltocene.[10] Compound **6** is also slightly more easily ionised than **1**; this suggests a considerably reduced HOMO–LUMO gap relative to that of **1** and its halogenated derivatives, which is consistent with calculated orbital energies (see Table S7 in Supporting Information) and with solution UV/Vis spectra, which show the onset of absorption for **6** to be approximately 1 eV lower than that of **1** or **7** (see Figure S5 in Supporting Information). To understand the relative importance of the structural features of **6** leading to the differences in IPs and EAs relative to **1**, we used DFT to calculate gas-phase IPs and EAs for the model compounds **6′** and **6″** (Table 2), in which the trifluoromethyl groups and the bis(trifluoromethyl)phenyl groups, respectively, are removed. These calculations show that the core tris(thieno)hexaazatriphenylene, **6″**, is both more easily oxidised and more easily reduced than **1**, in both cases by about 0.4 eV. This is consistent with DFT calculations of the IP and EA for thiophene and benzene, which show the former species is both more easily oxidised and more easily reduced (see Supporting Information). The more exothermic EA of **6″** versus **1** may also be related to the greater dominance of **A**-type resonance structures noted in the optimised structure of **6″** (vide supra), this being enforced by the bond-length distribution of thiophene. Comparison of the data for **6**, **6′** and **6″** shows that the bis(trifluoromethyl)phenyl groups affect both IP and EA; phenylation and addition of the CF₃ groups have opposing effects on the IP, but

work in concert to make the EA of **6** 1.3 eV more electronegative than that of **6″**.

Summary

In summary, we have synthesised several known and new hexaazatrinaphthylenes and a related tris(thieno)hexaazatriphenylene. We have shown that both the solid-state IPs and EAs of these materials can be tuned over ranges of nearly 2 eV through substitution. The results of DFT calculations indicate rather small reorganisation energies in these materials, suggesting low barriers to both electron and hole transport. The low barriers and highly exothermic electron affinities point towards potential applications as electron-transport materials in organic electronics. Finally, we have shown that one example adopts a π-stacked structure with a rather short π-stacking distance of 3.18 Å.

Experimental Section

Synthesis of literature hexaazatrinaphthylene derivatives: Compound **3a** was obtained according to the literature procedure;[6] details of the specific synthetic and purification methods used for **1** and **7** are given in the Supporting Information.

2,5-Bis-(3,5-bis-trifluoromethylphenyl)-3,4-dinitro-thiophene (S2): A mixture of 2,5-dibromo-3,4-dinitro-thiophene[54] (**S1**; 6.00 g, 18.08 mmol), 3,5-bis-trifluoromethyl-phenyl-tributyl-stannane (16.52 g, 36.15 mmol),[55] tris(dibenzylideneacetone) dipalladium (0.66 g, 0.72 mmol) and triphenylarsine (0.88 g, 2.88 mmol) in toluene (100 mL) was heated to 80 °C for 12 h under nitrogen. The mixture was cooled to room temperature and then a solution of potassium fluoride (30 mL, 2.0 M) was added. The mixture was stirred for 1 h. The organic layer was collected and the aqueous layer was extracted with diethyl ether. The combined organic layer was dried over magnesium sulfate and filtered. The solvent was removed under reduced pressure. The residue was crystallised from methanol to give a yellow solid (7.25 g, 67 % yield). ^{1}H NMR (300 MHz, [D]chloroform): $\delta = 8.08$ (br, 2H), 8.01 ppm (br, 4H); ^{13}C NMR (125 MHz, [D₆]acetone): $\delta = 140.0$, 138.7, 132.9 (q, J(C,F) = 34.0 Hz, C_o), 131.7, 131.4 (q, J(C,F) = 3.13 Hz, C_m), 127.2, 125.5 (septet, J(C,F) = 3.6 Hz, C_p), 124.0 ppm (q, J(C,F) = 271.7 Hz, CF₃); HRMS (EI): m/z calcd for C₂₀H₆F₁₂N₂O₄S 597.9857; found 597.9843; elemental analysis calcd (%) for C₂₀H₆F₁₂N₂O₄S: C 40.15, H 1.01, N 4.68; found: C 39.95, H 0.88, N 4.72.

2,5-Bis-(3,5-bis-trifluoromethylphenyl)thiophene-3,4-diamine (S3): A mixture of **S2** (2.22 g, 5.00 mmol) and tin(II) chloride dihydrate (11.28 g, 50.00 mmol) in ethanol (50 mL) was heated to reflux for 30 min under nitrogen atmosphere. After the mixture cooled to room temperature, it was poured onto ice. The solution was made slightly basic by the addition of 5 % aqueous sodium hydroxide solution. The solution was extracted with ethyl acetate. The combined organic layer was dried over magnesium sulfate. The solvent was removed under reduced pressure to give a solid. The solid was purified by flash chromatography on silica gel eluting with hexane/ethyl acetate (10:1) to give 1.60 g (59 %). ^{1}H NMR (300 MHz, [D₆]benzene): $\delta = 7.72$ (br s, 4H), 7.59 (br s, 2H), 2.62 ppm (br s, 4H); ^{13}C NMR (75 MHz, [D₆]benzene): $\delta = 136.6$, 135.1, 132.5 (q, J(C,F) = 33.0 Hz, C_m), 127.0 (m, C_o), 123.6 (q, J(C,F) = 270.9 Hz, CF₃), 120.1 (septet, J(C,F) = 4.5 Hz, C_p), 114.5 ppm; HRMS(EI): m/z calcd for C₂₀H₁₀F₁₂N₂S 538.0373; found 538.0379; elemental analysis calcd (%) for C₂₀H₁₀F₁₂N₂S: C 44.62, H 1.87, N 5.20; found: C 44.72, H 1.80, N 5.21.

Tris{2,5-bis(3,5-bis-trifluoromethyl-phenyl)thieno}[3,4-b,h,n]-1,4,5,8,9,12-hexaazatriphenylene (6): A mixture of hexaketocyclohexane octahydrate (0.296 g, 0.95 mmol) and **S3** (1.58 g, 2.85 mmol) was added to degassed

acetic acid (50 mL). The mixture was heated to 100 °C for 12 h under nitrogen atmosphere. After the mixture was cooled to room temperature, the solid was collected by filtration and was washed with acetic acid to give a black solid. The product was purified by flash chromatography on silica gel eluting with hexane/ethyl acetate (10:2) to give 1.00 g (63 %) of purified product. ^{1}H NMR (300 MHz, [D$_2$]dichloromethane) $\delta = 8.81$ (br, 12H), 7.96 ppm (br, 6H); HRMS (MALDI-TOF, CHCA matrix): m/z calcd for C$_{66}$H$_{18}$F$_{36}$N$_6$S$_3$, 1674.0180; found: 1674.0167; elemental analysis calcd (%) for C$_{66}$H$_{18}$F$_{36}$N$_6$S$_3$: C 47.32, H 1.08, N 5.02; found: C 47.35, H 0.99, N 5.14.

2,3,8,9,14,15-Hexafluoro-5,6,11,12,17,18-hexaazatrinaphthylene (8): A mixture of hexaketocyclohexane octahydrate (2.78 g, 8.90 mmol) and 4,5-difluoro-benzene-1,2-diamine[13,14] (3.85 g, 26.71 mmol) was added to deoxygenated acetic acid (250 mL). The mixture was refluxed for 16 h. After the mixture was cooled to room temperature, the solid was collected by filtration and was washed with acetic acid to give a yellow solid (2.88 g, 58 % crude yield). Gradient sublimation at high vacuum (ca. 250 °C) gave fine needle-like microcrystals, which, however, did not give satisfactory elemental analysis. ^{1}H NMR (300 MHz, [D]chloroform/ [D]trifluoroacetic acid): $\delta = 8.42$ ppm (t, J(H,F) = 8.5 Hz, 6H); ^{19}F NMR (376.3 MHz, [D]chloroform/[D]trifluoroacetic acid): $\delta = -121.26$ ppm (t, J(F,H) = 8.5 Hz); HRMS(EI): m/z calcd for C$_{24}$H$_6$F$_6$N$_6$ 492.0558; found 492.0585; elemental analysis calcd (%) for C$_{24}$H$_6$F$_6$N$_6$: C 58.55, H 1.23, N 17.07, F 22.34; found: C 56.98, H 1.39, N 16.81, F 22.36.

1,2,3,4,7,8,9,10,13,14,15,16-Dodecafluoro-5,6,11,12,17,18-hexaazatrinaphthylene (9): A mixture of hexaketocyclohexane octahydrate (2.50 g, 9.25 mmol) and 3,4,5,6-tetrafluoro-benzene-1,2-diamine[15,16] (5.00 g, 27.76 mmol) was added to deoxygenated acetic acid (150 mL). The mixture was refluxed for 12 h under nitrogen. After the mixture was cooled to room temperature, the resulting solid was collected by filtration and was washed with acetic acid to give a yellow solid (4.05 g, 73 % crude yield). A portion was purified by gradient sublimation at high vacuum (ca. 250 °C) to give yellow crystals, which were not soluble in common organic solvents including CF$_3$CO$_2$H. However, the crystals were soluble in concentrated sulfuric acid. ^{19}F NMR (376.3 MHz, [D$_2$]sulfuric acid): $\delta = -123.53$, -138.35 ppm; HRMS(EI): m/z calcd for C$_{24}$F$_{12}$N$_6$: 599.9993; found 599.9981; elemental analysis calcd (%) for C$_{24}$F$_{12}$N$_6$: C 48.02, H 14.00; found: C 48.03, H 14.10.

PES and IPES measurements: The organic thin films were grown and characterised with PES and IPES under UHV without any exposure to air. The substrates were Si wafers covered with a 50 Å Ti layer (for adhesion) and a 1200 Å Au layer that had been previously degreased by boiling in acetone and methanol. Compounds **1**, **6**, **7** and **9** were thermally evaporated from pyrolytic boron nitride crucibles after an extensive outgassing procedure. Films with thickness of 80 Å were deposited on the Au surface at a rate of 1–2 Å s^{-1}. Film deposition was monitored using a quartz crystal microbalance, assuming the same density of 1.5 g cm^{-3} for all four derivatives. Compound **3a** could not withstand thermal evaporation and was spin-coated (6000 rpm for 60 s) from a 0.08 wt % solution of dichloromethane in a nitrogen-purged glove box (humidity < 5 %). The film was then dried from solvent at 50 °C for one hour under nitrogen. The thickness of the film prepared by spin coating was not measured but was assumed to be less than 100 Å. Ambient exposure of the **3a** film was unavoidable when loading the sample into the chamber, but was limited to less than a minute.

The PES was performed with a He discharge lamp by using the He I (21.22 eV) and He II (40.8 eV) photon lines with a total experimental resolution of 150 meV. The IPES was carried out in the isochromat mode by using a fixed-photon-energy detector centred at 9.2 eV and an electron gun, resulting in a combined resolution of 500 meV. The IPES electron beam current density was limited to around 1×10^{-6} A cm^{-2} to minimise degradation of the organic thin film. In all cases, we performed the PES experiment first, then the IPES measurement, and repeated the PES to assess any electron-beam-induced degradation.

The PES and IPES energy scales were aligned by using the position of the Fermi step measured on a gold substrate. The position of the vacuum level (E_{vac}) was measured on each sample using the onset of photoemission. The experimental values for IP and EA correspond to the energy difference between E_{vac} and the leading edge of the HOMO and LUMO feature, respectively.

Crystal structure of 7: Yellow single crystals of **7** were obtained during purification by vacuum sublimation. A $0.45 \times 0.30 \times 0.20$ mm crystal was selected and data collected at 96 K using a Bruker SMART diffractometer with CCD detector with Mo$_{K\alpha}$ radiation (0.71073 Å). The crystal was found to belong to the monoclinic space group $P2_1/c$ with $a = 10.9644(11)$, $b = 26.634(3)$, $c = 8.0161(8)$ Å, $\beta = 108.908(2)°$, $Z = 4$, $F_{000} = 1176$, $\mu_{calcd} = 0.807$ mm^{-1}, $\rho_{calcd} = 1.773$ g cm^{-3}. Least-squares refinement of F^2 was carried out using all 6478 independent reflections measured (4050 with $[I > 2\sigma(I)]$); refinement converged with $R = 0.828$ and $wR = 0.1126$ (all data). CCDC-620134 contains the supplementary crystallographic data for this paper. These data can be obtained free of charge from The Cambridge Crystallographic Data Centre via www.ccdc.cam.ac.uk/data_request/cif.

DFT calculations: Molecular geometries were optimised in the neutral, radical anion and radical cation states, by means of density functional theory (DFT) using the B3LYP functionals, in which Becke's three-parameter hybrid exchange functional[56,57] was combined with the Lee-Yang-Parr correlation functional,[58] and a 6-31G** split valence plus double polarisation basis set. Ionisation energies, electron affinities and reorganisation energies were calculated from direct calculation of the energies of the relevant points on the potential-energy surfaces. Specifically, vertical IPs were calculated as the energy difference between the energy of the cation at neutral geometry and the neutral molecule at neutral geometry and adiabatic IPs as the difference between the cation at the relaxed cation geometry and the neutral molecule at neutral geometry. The difference between vertical and adiabatic IPs corresponds to the relaxation energy, λ_2, associated with the cation surface. The parameter λ_1 is defined as the difference between the neutral species at the cation geometry. The sum of λ_1 and λ_2, λ_i is the Marcus intramolecular reorganisation energy for the self-exchange reaction of a molecule and its cation. Similarly, vertical and adiabatic EAs were calculated as the difference between the energy of the anion at neutral geometry and the neutral species at neutral geometry and as the energy difference between the relaxed anion and neutral molecule, respectively. The relevant λ_2 contributing to λ_i for self-exchange between a molecule and its cation is then the difference between vertical and adiabatic EAs, while λ_1 is the energy difference between the anion at neutral geometry and at anion geometry. All DFT calculations were carried out with the Gaussian suite of programs (both Gaussian 98, revision A.11[59] and Gaussian 03[60]).

Acknowledgements

[1] H. Bock, A. Babeau, I. Seguy, P. Jolinat, P. Destruel, *ChemPhysChem* **2002**, *3*, 532.

[2] B. R. Kaafarani, T. Kondo, J. Yu, Q. Zhang, D. Dattilo, C. Risko, S. C. Jones, S. Barlow, B. Domercq, F. Amy, A. Khan, J. L. Brédas, B. Kippelen, S. R. Marder, *J. Am. Chem. Soc.* **2005**, *127*, 16358.

[3] G. Kestemont, V. de Halleux, M. Lehmann, D. A. Ivanov, M. Watson, Y. H. Geerts, *Chem. Commun.* **2001**, 2074.

[4] V. Lemaur, D. A. de Silva Filho, V. Coropceanu, M. Lehmann, Y. Geerts, J. Piris, M. G. Debije, A. M. van de Craats, K. Senthilkumar, L. D. Siebbeles, J. M. Warman, J. L. Brédas, J. Cornil, *J. Am. Chem. Soc.* **2004**, *126*, 3271.

[5] X. Crispin, J. Cornil, R. Friedlein, K. K. Okudaira, V. Lemaur, A. Crispin, G. Kestemont, M. Lehmann, M. Fahlman, R. Lazzaroni, Y. Geerts, G. Wendin, N. Ueno, J. L. Brédas, W. R. Salaneck, *J. Am. Chem. Soc.* **2004**, *126*, 11889.

[6] M. Lehmann, G. Kestemont, R. G. Aspe, C. Buess-Herman, M. H. J. Koch, M. G. Debije, J. Piris, M. P. de Haas, J. M. Warman, M. D. Watson, V. Lemaur, J. Cornil, Y. H. Geerts, R. Gearba, D. A. Ivanov, *Chem. Eur. J.* **2005**, *11*, 3349.

[7] C. W. Ong, S.-C. Liao, T. H. Chang, H.-F. Hsu, *Tetrahedron Lett.* **2003**, *44*, 1477.

[8] C. W. Ong, S.-C. Liao, T. H. Chang, H.-F. Hsu, *J. Org. Chem.* **2004**, *69*, 3181.

[9] T. Ishi-i, K. Yaguma, R. Kuwahara, Y. Taguri, S. Mataka, *Org. Lett.* **2006**, *8*, 585.

[10] C. K. Chan, F. Amy, Q. Zhang, S. Barlow, S. R. Marder, A. Kahn, *Chem. Phys. Lett.* **2006**, *431*, 67.

[11] S. Skujins, G. A. Webb, *Tetrahedron* **1969**, *25*, 3935.

[12] M. Du, X.-H. Bu, K. Biradha, *Acta Crystallogr. Sect. C* **2001**, *57*, 199.

[13] S. K. Kotovskaya, N. M. Perova, Z. M. Baskakova, S. A. Romanova, V. N. Charushin, O. N. Chupakhin, *Zh. Org. Khim.* **2001**, *37*, 598.

[14] R. B. Baudy, L. P. Greenblatt, I. L. Jirkovsky, M. Conklin, R. J. Russo, D. R. Bramlett, T. A. Emrey, J. T. Simmonds, D. M. Kowal, R. P. Stein, R. P. Tasses, *J. Med. Chem.* **1993**, *36*, 331.

[15] A. Heaton, M. Hill, F. Drakesmith, *J. Fluorine Chem.* **1997**, *81*, 133.

[16] J. F. W. Keana, S. M. Kher, S. X. Cai, C. M. Dinsmore, A. G. Glenn, J. Guastella, J. Huang, V. Ilyin, Y. Lu, P. L. Mouser, R. M. Woodward, E. Weber, *J. Med. Chem.* **1995**, *38*, 4367.

[17] We were unable to obtain **8** analytically pure and so did not obtain PES and IPES spectra.

[18] M. Alfonso, H. Stoeckli-Evans, *Acta Crystallogr. Sect. E* **2001**, *57*, 0242.

[19] Bond lengths from the structure of [Ag₃(**1**)]-[PF₆]₃·0.75 CHCl₃·2.25 MeCN (X.-H. Bu, K. Biradha, T. Yamaguchi, M. Nishimura, T. Ito, K. Tanaka, M. Shionoya, *Chem. Commun.* **2000**, 1953) are not included, since these were rather imprecisely determined.

[20] The structures of the radical ions of **6**, in which there are a large number of degrees of freedom, could not be successfully minimised. Accordingly, we were also unable to calculate reorganisation energies and adiabatic values of IP and EA for this compound.

[21] R. A. Marcus, *J. Chem. Phys.* **1956**, *24*, 966.

[22] For example, see: R. D. Hreha, C. P. George, A. Haldi, B. Domercq, M. Malagoli, S. Barlow, J.-L. Brédas, B. Kippelen, S. R. Marder, *Adv. Funct. Mater.* **2003**, *13*, 967. While the barrier is strictly ΔH^+, ΔS^+ can be neglected due to similar vibrational degrees of freedom associated with the two adiabatic surfaces, meaning $\lambda/4$ is also a good estimate of the free-energy barrier, ΔG^+.

[23] The reorganisation energy can also be obtained from a full vibrational analysis through summation of the contributions of the vibrational modes involved (R. A. Marcus, N. Sutin, *Biochim. Biophys. Acta* **1985**, *811*, 265).

[24] M. Malagoli, J.-L. Brédas, *Chem. Phys. Lett.* **2000**, *327*, 13.

[25] B. C. Lin, C. P. Cheng, Z.-Q. You, C.-P. Hsu, *J. Am. Chem. Soc.* **2005**, *127*, 66.

[26] X. Zhan, C. Risko, F. Amy, C. Chan, W. Zhao, S. Barlow, A. Kahn, J.-L. Brédas, S. R. Marder, *J. Am. Chem. Soc.* **2005**, *127*, 9021.

[27] F. Garnier, G. Horowitz, D. Fichou, A. Yassar, *Synth. Met.* **1996**, *81*, 163.

[28] H. E. Katz, Z. Bao, *J. Phys. Chem. B* **2000**, *104*, 671.

[29] R. C. Haddon, X. Chi, M. E. Itkis, J. E. Anthony, D. L. Eaton, T. Siegrist, C. C. Mattheus, T. T. M. Palstra, *J. Phys. Chem. B* **2002**, *106*, 8288.

[30] Y. Olivier, V. Lemaur, J. L. Brédas, J. Cornil, *J. Phys. Chem. A* **2006**, *110*, 6356.

[31] A. M. van de Craats, N. Stutzmann, O. Bunk, M. M. Nielsen, M. Watson, K. Müllen, H. D. Chanzy, H. Sirringhaus, R. H. Friend, *Adv. Mater.* **2003**, *15*, 495.

[32] Z. An, J. Yu, S. C. Jones, S. Barlow, S. Yoo, B. Domercq, P. Prins, L. D. A. Siebbeles, B. Kippelen, S. R. Marder, *Adv. Mater.* **2005**, *17*, 2580.

[33] K. O. Sylvester-Hvid, *J. Phys. Chem. B* **2006**, *110*, 2618.

[34] A. R. Murphy, J. S. Liu, C. Luscombe, D. Kavulak, J. M. J. Fréchet, R. J. Kline, M. D. McGehee, *Chem. Mater.* **2005**, *17*, 4892.

[35] H. Xu, Y. Wang, G. Yu, W. Xu, Y. B. Song, D. Q. Zhang, Y. Q. Liu, D. B. Zhu, *Chem. Phys. Lett.* **2005**, *414*, 369.

[36] J. E. Anthony, J. S. Brooks, D. L. Eaton, S. R. Parkin, *J. Am. Chem. Soc.* **2001**, *123*, 9482.

[37] X.-C. Li, H. Sirringhaus, F. Garnier, A. B. Holmes, S. C. Moratti, N. Feeder, W. Clegg, S. J. Teat, R. H. Friend, *J. Am. Chem. Soc.* **1998**, *120*, 2206.

[38] J. E. Anthony, D. L. Eaton, S. R. Parkin, *Org. Lett.* **2002**, *4*, 15.

[39] K. Kobayashi, R. Shimaoka, M. Kawahata, M. Yamanaka, K. Yamaguchi, *Org. Lett.* **2006**, *8*, 2385.

[40] A. M. van de Craats, J. M. Warman, H. Hasebe, R. Naito, K. Ohta, *J. Phys. Chem. B* **1997**, *101*, 9224.

[41] S. Kumar, D. S. S. Rao, S. K. Prasad, *J. Mater. Chem.* **1999**, *9*, 2751.

[42] R. I. Gearba, M. Lehmann, J. Levin, D. A. Ivanov, M. H. J. Koch, J. Barberá, M. G. Debije, J. Piris, Y. H. Geerts, *Adv. Mater.* **2003**, *15*, 1614.

[43] This type of estimate assumes that the analyte and reference redox system show comparable solvation energies and comparable solid-state polarisation effects and ideally requires more or less reversible electrochemistry to ensure that the observed potential represents the thermodynamic potential. Moreover, differences in the magnitudes of solvation energies and solid-state polarisation effects mean that IPs are best estimated from M⁺/M redox couples and a known IP, while EAs are best estimated from M/M⁻ and a known EA. For example, we recently found that, in the case of 1,1-diaryl-2,3,4,5-tetraphenylsiloles, use of [silole]/[silole]⁻ potentials, the TPD⁺/TPD potential and the IP of TPD gave EAs almost 1 eV more exothermic than the values obtained by direct measurement. See reference [26].

[44] L. Segev, A. Salomon, A. Natan, D. Cahen, L. Kronik, F. Amy, C. K. Chan, A. Kahn, *Phys. Rev. B* **2006**, *74*, 165323/1.

[45] F. Amy, C. K. Chan, W. Zhao, J. Hyung, A. Kahn, M. Ono, N. Ueno, D. Cahen, L. Kronik, G. Nesher, A. Salomon, L. Segev, O. Seitz, H. Shpaisman, A. Schöll, E. Umbach, *J. Phys. Chem. B* **2006**, *110*, 21826.

[46] N. Sato, H. Inokuchi, E. A. Silinish, *Chem. Phys.* **1987**, *115*, 269.

[47] J. D. Anderson, E. M. McDonald, P. A. Lee, M. L. Anderson, E. L. Ritchie, H. K. Hall, T. Hopkins, E. A. Nash, J. Wang, A. Padias, S. Thayumanavan, S. Barlow, S. R. Marder, G. Jabbour, S. Shaheen, B. Kippelen, N. Peyghambarian, R. M. Wightman, N. R. Armstrong, *J. Am. Chem. Soc.* **1998**, *120*, 9646.

[48] W. Y. Gao, A. Kahn, *J. Appl. Phys.* **2003**, *94*, 359.

[49] A. Kahn, N. Koch, W. Gao, *J. Polym. Sci. Part B* **2003**, *41*, 2529–2548.

[50] D. Cahen, A. Kahn, *Adv. Mater.* **2003**, *15*, 271.

[51] These values are taken from J. E. Huheey, E. A. Keiter, R. L. Keiter, *Inorganic Chemistry: Principles of Structure and Reactivity*, 4th ed., Harper Collins, New York, **1993**, p. 187, in which values according to a variety of other scales are also given.

[52] R. Dudde, B. Reihl, A. Otto, *J. Chem. Phys.* **1990**, *92*, 3930.

[53] The competing inductive and resonance effects of F and Cl can of course be gauged by Hammett coefficients. See for example J. March, *Advanced Organic Chemistry*, 3rd ed., Wiley, New York, **1985**.

[54] D. D. Kenning, K. A. Mitchell, T. R. Calhoun, M. R. Funfar, D. J. Sattler, S. C. Rasmussen, *J. Org. Chem.* **2002**, *67*, 9073.

[55] R. G. Kultyshev, G. K. S. Prakash, G. A. Olah, J. W. Faller, J. Parr, *Organometallics* **2004**, *23*, 3184.

[56] A. D. Becke, *Phys. Rev. A* **1988**, *38*, 3098.

[57] A. D. Becke, *J. Chem. Phys.* **1993**, *98*, 5648.

[58] C. T. Lee, W. T. Yang, R. G. Parr, *Phys. Rev. B* **1988**, *37*, 785.

[59] Gaussian 98 (Revision A.11), M. J. Frisch, G. W. Trucks, H. B. Schlegel, G. E. Scuseria, M. A. Robb, J. R. Cheeseman, V. G. Zakrzewski, J. A. Montgomery, R. E. Stratmann, J. C. Burant, S. Dapprich, J. M. Millam, A. D. Daniels, K. N. Kudin, M. C. Strain, O. Farkas, J. Tomasi, V. Barone, M. Cossi, R. Cammi, B. Mennucci, C. Pomelli, C. Adamo, S. Clifford, J. Ochterski, G. A. Petersson, P. Y. Ayala, Q. Cui, K. Morokuma, D. K. Malick, A. D. Rabuck, K. Raghavachari,

J. B. Foresman, J. Cioslowski, J. V. Ortiz, B. B. Stefanov, G. Liu, A. Liashenko, P. Piskorz, I. Komaromi, R. Gomperts, R. L. Martin, D. J. Fox, T. Keith, M. A. Al-Laham, C. Y. Peng, A. Nanayakkara, C. Gonzalez, M. Challacombe, P. M. W. Gill, B. G. Johnson, W. Chen, M. W. Wong, J. L. Andres, M. Head-Gordon, E. S. Replogle, J. A. Pople, Gaussian, Inc., Pittsburgh, PA, **1998**.

[60] Gaussian 03, Revision B.05, M. J. Frisch, G. W. Trucks, H. B. Schlegel, G. E. Scuseria, M. A. Robb, J. R. Cheeseman, J. A. Montgomery, Jr., T. Vreven, K. N. Kudin, J. C. Burant, J. M. Millam, S. S. Iyengar, J. Tomasi, V. Barone, B. Mennucci, M. Cossi, G. Scalmani, N. Rega, G. A. Petersson, H. Nakatsuji, M. Hada, M. Ehara, K. Toyota, R. Fukuda, J. Hasegawa, M. Ishida, T. Nakajima, Y. Honda, O. Kitao, H. Nakai, M. Klene, X. Li, J. E. Knox, H. P. Hratchian, J. B. Cross, V. Bakken, C. Adamo, J. Jaramillo, R. Gomperts, R. E. Stratmann, O. Yazyev, A. J. Austin, R. Cammi, C. Pomelli, J. W. Ochterski, P. Y. Ayala, K. Morokuma, G. A. Voth, P. Salvador, J. J. Dannenberg, V. G. Zakrzewski, S. Dapprich, A. D. Daniels, M. C. Strain, O. Farkas, D. K. Malick, A. D. Rabuck, K. Raghavachari, J. B. Foresman, J. V. Ortiz, Q. Cui, A. G. Baboul, S. Clifford, J. Cioslowski, B. B. Stefanov, G. Liu, A. Liashenko, P. Piskorz, I. Komaromi, R. L. Martin, D. J. Fox, T. Keith, M. A. Al-Laham, C. Y. Peng, A. Nanayakkara, M. Challacombe, P. M. W. Gill, B. Johnson, W. Chen, M. W. Wong, C. Gonzalez, J. A. Pople, Gaussian, Inc., Wallingford CT, **2004**.